A&A 481, 229–233 (2008)
DOI: 10.1051/0004-6361:20079058

Astronomy & Astrophysics

Chromospheric features of LQ Hydrae from Hα line profiles

A. Frasca[1], Zs. Kővári[2], K. G. Strassmeier[3], and K. Biazzo[1]

[1] INAF - Catania Astrophysical Observatory, via S. Sofia 78, 95123 Catania, Italy
e-mail: [antonio.frasca;katia.biazzo]@oact.inaf.it
[2] Konkoly Observatory, 1525 Budapest, PO Box 67, Hungary
e-mail: kovari@konkoly.hu
[3] Astrophysical Institute Potsdam, An der Sternwarte 16, 14482 Potsdam, Germany
e-mail: kstrassmeier@aip.de

Received 13 November 2007 / Accepted 3 January 2008

ABSTRACT

We analyze the Hα spectral variability of the rapidly-rotating K1-dwarf LQ Hya using high-resolution Hα spectra recorded during April–May 2000. Chromospheric parameters were computed from the Hα profile as a function of rotational phase. We find that all these parameters vary in phase, with a higher chromospheric electron density coinciding with the maximum Hα emission. We find a clear rotational modulation of the Hα emission that is better emphasized by subtracting a reference photospheric template built up with a spectrum of a non-active star of the same spectral type. A geometrical plage model applied to the Hα variation curve allows us to derive the location of the active regions that come out to be close in longitude to the most pronounced photospheric spots found with Doppler imaging applied to the photospheric lines in the same spectra. Our analysis suggests that the Hα features observed in LQ Hya in 2000 are a scaled-up version of the solar plages as regards dimensions and/or flux contrast. No clear indication of chromospheric mass motions emerges.

Key words. stars: activity – stars: late-type – stars: chromospheres – stars: starspots – stars: individual: LQ Hydrae

1. Introduction

According to the solar-stellar analogy, chromospheric stellar activity can be established by the presence of emission in the core of the Balmer Hα line. As in the Sun, Hα emission intensification has often been observed in surface features (plages) spatially connected with the photospheric starspots (see, e.g., Catalano et al. 2000; Biazzo et al. 2006, 2007, and references therein). Thus, the time variability of the Hα spectral features can be used to estimate the basic properties of the emitting sources, allowing the geometry of the stellar chromosphere to be mapped.

In this paper we analyze the Hα spectral variability of the young, rapidly-rotating ($P_{\rm rot} \approx 1.6$ d) single K2-dwarf LQ Hydrae (HD 82558 = Gl 355) using 15 high-resolution spectra recorded during April–May 2000. All Hα spectra were acquired simultaneously with the mapping lines used for the year-2000 Doppler imaging study presented in our previous paper (Kővári et al. 2004, hereafter Paper I). LQ Hya was first recognized as a chromospherically active star through Ca II H&K emission (Bidelman 1981; Heintz 1981). The Hα absorption filled in by chromospheric emission was reported first by Fekel et al. (1986), and LQ Hya was classified as a BY Dra-type spotted star. Variable Hα emission-peak asymmetry was investigated by Strassmeier et al. (1993, hereafter Paper II), who attributed it to the presence of chromospheric velocity fields in the Hα forming layer probably surrounding photospheric spots.

In our spectroscopic study in Paper I, we presented Doppler images using the Fe I-6411, Fe I-6430, and Ca I-6439 lines for both the late April data and the early May 2000 dataset. Doppler imaging was supported by simultaneous photometric measurements in Johnson-Cousins *VI* bands. Doppler images showed spot activity uniformly at latitudes between −20°and +50°, sometimes with high-latitude appendages, but without a polar spot. Comparing the respective maps from two weeks apart, rapid spot evolution was detected, which was attributed to strong cross-talks between the neighboring surface features through magnetic reconnections. In Table 1 we give a summary of the stellar parameters as they emerged from Paper I.

Table 1. Astrophysical data for LQ Hya (adopted from Kővári et al. 2004).

Parameter	Value
Classification	K2 V
Distance (Hipparcos)	18.35 ± 0.35 pc
$(B-V)_{\rm Hipparcos}$	0.933 ± 0.021 mag
$(V-I)_{\rm Hipparcos}$	1.04 ± 0.02 mag
Luminosity, L	$0.270 \pm 0.009\ L_\odot$
log g	4.0 ± 0.5
$T_{\rm eff}$	5070 ± 100 K
$v \sin i$	28.0 ± 1.0 km s^{-1}
Inclination, i	$65° \pm 10°$
Period, $P_{\rm rot}$	1.60066 ± 0.00013 days
Radius, R	$0.97 \pm 0.07\ R_\odot$
Mass	$\approx 0.8\ M_\odot$
Age	≈ZAMS

The observations are again briefly presented in Sect. 2 and the method used for the Hα spectral study is described in Sect. 3. The results are presented in Sect. 4. Since the Hα observations of this paper were included in the spectroscopic data used in Paper I to reconstruct the year-2000 Doppler images, in Sect. 5 we take the opportunity to compare the photospheric features with the contemporaneous Hα-emitting regions.

Table 2. Observing log and radial velocities.

HJD	Phase	v_r (km s^{-1})	σ_{v_r} (km s^{-1})
2 451 639.681	0.187	7.1	0.6
2 451 640.647	0.791	7.8	0.6
2 451 641.648	1.416	8.6	0.5
2 451 642.662	2.050	7.4	0.6
2 451 643.744	2.726	7.6[a]	2.4
2 451 644.677	3.309	8.3	0.6
2 451 660.683	13.308	8.8	0.5
2 451 661.668	13.924	8.7	0.6
2 451 662.652	14.538	9.5	0.6
2 451 663.654	15.165	7.5	0.5
2 451 664.667	15.798	9.0	0.6
2 451 665.653	16.413	9.8	0.5
2 451 666.661	17.043	8.0	0.5
2 451 667.665	17.670	7.4	0.6
2 451 668.670	18.298	8.1	0.7

[a] With 16 Vir as RV standard.

2. Spectroscopic observations

The series of 15 Hα spectra was collected, one spectrum per night, during two observing runs (April 4–9, 2000, and April 25–May 3, 2000) at the Kitt Peak National Observatory (KPNO) with the 0.9 m coudé-feed telescope. The 3096 × 1024 F3KB CCD detector was employed, together with grating A, camera 5, and the long collimator. The spectra were centered at 6500 Å with a wavelength range of 300 Å. The effective resolution was ≈28 000 (11 km s^{-1}). We achieved signal-to-noise ratios (S/N) of about 250 in 45-min integration time, with the only exception being the spectrum at 2.726 phase for which an S/N of just 50 could be reached due to bad sky conditions.

The mean HJDs of the observations, the phases, as well as the radial velocities, are summarized in Table 2. For phasing the spectra, HJD = 2 448 270.0 + 1.600656 × E was used, where the arbitrarily chosen zero point is the same as used for our former Doppler imaging studies (Strassmeier et al. 1993; Kővári et al. 2004). As radial velocity (RV) standard star, β Gem (v_r = 3.23 km s^{-1}) was measured, except for HJD 2 451 643.744 when 16 Vir (v_r = 36.48 km s^{-1}) was observed (Scarfe et al. 1990). For more details we refer to Paper I.

3. Data analysis

The Balmer Hα line is a useful and easily accessible indicator of chromospheric activity in the optical spectrum. It has been proven to be very effective for detecting chromospheric plages both in the Sun and in active stars, due to its high contrast against the surrounding chromosphere (see, e.g., Frasca et al. 1998; Biazzo et al. 2006, 2007).

However, the Hα line is formed in a wide depth range in the stellar atmosphere, ranging from the temperature minimum to the upper chromosphere. To extract the chromospheric contribution from the line core, we apply a method usually called "spectral synthesis", which consists in the subtraction of synthetic spectra or of observed spectra of non-active standard stars (reference spectra) (see, e.g., Herbig 1985; Barden 1985; Frasca & Catalano 1994; Montes et al. 1995). The difference between observed and reference spectra provides the net Hα emission, which can be integrated to estimate the total radiative chromospheric loss in the line.

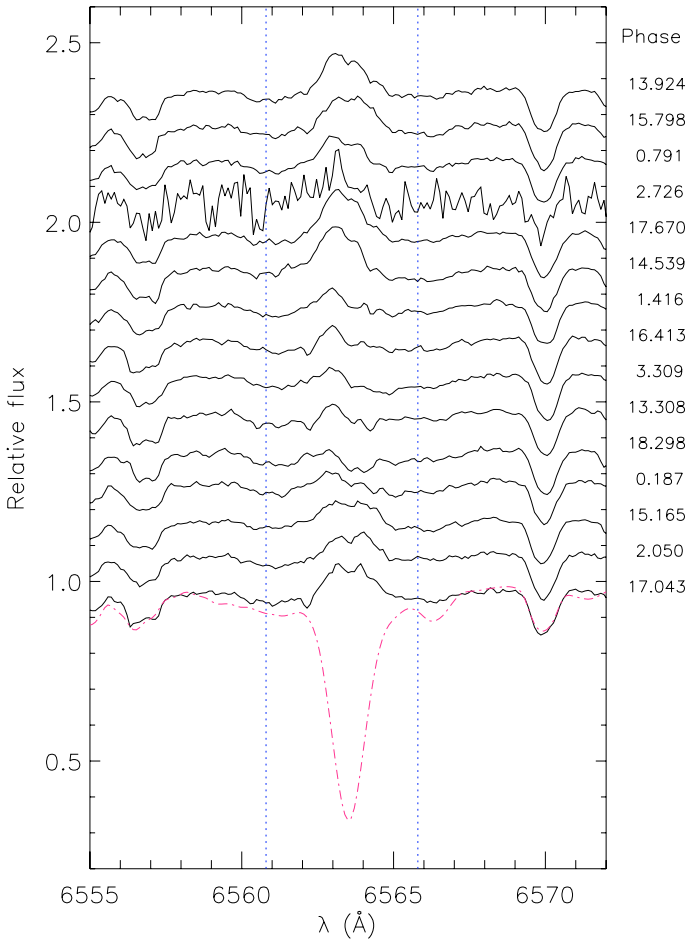

Fig. 1. Time series of Hα profiles for LQ Hya in April–May 2000 sorted in phase order. The non-active template built up with a spectrum of the non-active, slowly-rotating K2 V star HD 3765 is shown by a dash-dotted line at the bottom. The vertical dotted lines mark the integration interval for the *raw* Hα equivalent width ($EW_{H\alpha}$).

We point out that one can obtain the true chromospheric Hα emission with this method only if the chromosphere is also optically thin inside the active regions or if the plages are not extended enough to appreciably affect the photospheric spectrum. In the opposite case, the subtraction of the underlying photospheric profile would overestimate the Hα chromospheric emission.

For this reason we have also measured the Hα equivalent width in the observed spectra ($EW_{H\alpha}$), fixing a constant integration window of 5.0 Å, i.e. integrating the emission core inside the absorption wings (see Fig. 1). The net Hα equivalent width, $\Delta EW_{H\alpha}$, was instead measured in the residual spectra obtained from the original ones with the "spectral synthesis" method. The non-active template was built using a high-resolution (R = 42 000) spectrum of the K2 V star HD 3765 retrieved from the ELODIE archive. We chose HD 3765 because its spectral type and color index $B - V$ = 0.942 (Weis 1996) are nearly identical with those of LQ Hya, because its rotation velocity is very low ($v \sin i$ = 2.5 km s^{-1}, Strassmeier et al. 2000), and because it has a low level of magnetic activity compared to LQ Hya. The spectrum was first degraded to the resolution of the KPNO spectra by convolving it with a Gaussian kernel and subsequently broadened by convolution with a rotational profile corresponding to the $v \sin i$ of 28 km s^{-1} of LQ Hya.

Table 3. Equivalent widths of the *raw* ($EW_{H\alpha}$) and the *residual* spectra ($\Delta EW_{H\alpha}$), errors of the equivalent widths (σ_{EW}), and velocity shifts ΔV_{em} and ΔV_{em}^{res} for the *raw* and the *residual* spectra, respectively.

Phase	$EW_{H\alpha}$ (Å)	$\Delta EW_{H\alpha}$ (Å)	σ_{EW} (Å)	ΔV_{em} (km s^{-1})	ΔV_{em}^{res} (km s^{-1})
0.187	0.172	0.934	0.041	−27.46	−1.78
0.791	0.117	1.003	0.038	−14.05	−0.13
1.416	0.183	0.935	0.036	−29.11	−0.96
2.050	0.107	1.013	0.043	7.40	−1.29
2.726	0.116	1.045	0.213	−17.00	−5.80
3.309	0.239	0.879	0.037	−32.70	−2.92
13.308	0.248	0.858	0.044	−28.68	−2.19
13.924	0.058	1.045	0.048	−10.77	1.38
14.538	0.025	1.050	0.041	−20.01	−1.38
15.165	0.099	0.998	0.041	−0.69	−0.56
15.798	0.073	1.050	0.036	−1.87	1.09
16.413	0.215	0.919	0.035	−29.60	−0.49
17.043	0.094	1.024	0.034	−0.18	0.65
17.670	0.038	1.074	0.051	−13.38	0.36
18.298	0.325	0.834	0.038	−43.07	0.29

The error of the equivalent width, σ_{EW}, was evaluated by multiplying the integration range by the photometric error on each point. This was estimated by the standard deviation of the observed flux values on the difference spectra in two spectral regions near the Hα line. The values of $EW_{H\alpha}$, $\Delta EW_{H\alpha}$, and σ_{EW} are reported in Table 3.

We also measured the central wavelength of the Hα emission both in the raw (observed) and residual spectra by evaluating the centroid of the core emission. This quantity provided us with the radial velocity shifts between the Hα emission and the photosphere measured both in the raw (ΔV_{em}) and in the residual spectra (ΔV_{em}^{res}). The values of ΔV_{em} and ΔV_{em}^{res} are reported in Table 3 as well.

4. Results

In the LQ Hya spectra, the Hα line is a strongly variable feature displaying absorption wings and a core changing from a completely filled-in configuration to a moderate emission above the continuum (see Fig. 1). A faint single peak just filling in the line core, without reaching the continuum, is observed at the phases of minimum Hα emission (ϕ = 0.2–0.4), whereas double-peaked emission profiles are observed with a central reversal at the other phases. The "blue" emission peak is often stronger than the "red" one, although at some phases, nearly equal peak heights and even reversed intensity ratios are also observed. The Hα profiles are shown in Fig. 1 along with the photospheric template built up with an HD 3765 spectrum (see Sect. 3).

We estimated the chromospheric electron density in LQ Hya adopting the assumptions from Paper II, i.e. an isothermal chromosphere with T_{chrom} = 10 000 K for which the optical depth in the Hα center can be derived by the formulation of Cram & Mullan (1979):

$$\ln \tau_{chrom} = \left(\frac{\Delta\lambda_{peak}}{2\Delta\lambda_D}\right)^2, \quad (1)$$

where $\Delta\lambda_{peak}$ is the wavelength separation of the blue and red emission peaks, and $\Delta\lambda_D$ = 0.28 Å is the chromospheric Doppler width. We measured $\Delta\lambda_{peak}$ on the observed spectra by fitting two Lorentzian functions to all the double-peaked Hα profiles. Obviously, this analysis could not be applied to the single-peaked spectra close to the minimum emission at phase 0.2–0.5. Combining Eqs. (8) and (14) in Cram & Mullan (1979), the electron density n_e in cm^{-3} can be evaluated as

$$n_e = 1.67 \times 10^{14} \frac{F_{max}}{F_{cont}} \frac{B(T_{eff})}{B(T_{chrom})} \tau_{chrom}^{-1}, \quad (2)$$

where $\frac{F_{max}}{F_{cont}}$ is the ratio of the Hα peak to the continuum flux, as measured on our spectra, and B is the Planck function calculated for the effective temperature of LQ Hya (T_{eff} = 5100 K) and at T_{chrom} = 10 000 K. The optical depth at the Hα center changes from about 30 to 4 and the electron density from 5×10^{11} to 4×10^{12} cm^{-3} from phase ≈0.2 (near the minimum Hα emission) to the phases of maximum emission (ϕ = 0.6–0.8, see Fig. 2). In the same figure, the flux ratio between the red and the blue peaks $\frac{F_R}{F_V}$ and the peak separation $\Delta\lambda_{peak}$ are plotted versus the rotational phase. All these quantities appear modulated by the stellar rotation. Symmetric profiles ($\frac{F_R}{F_V} \simeq 1$) tend to be observed when the most active regions, judging from the photospheric spot contrast, are in the visible hemisphere, similar to what was found by Strassmeier et al. in Paper II.

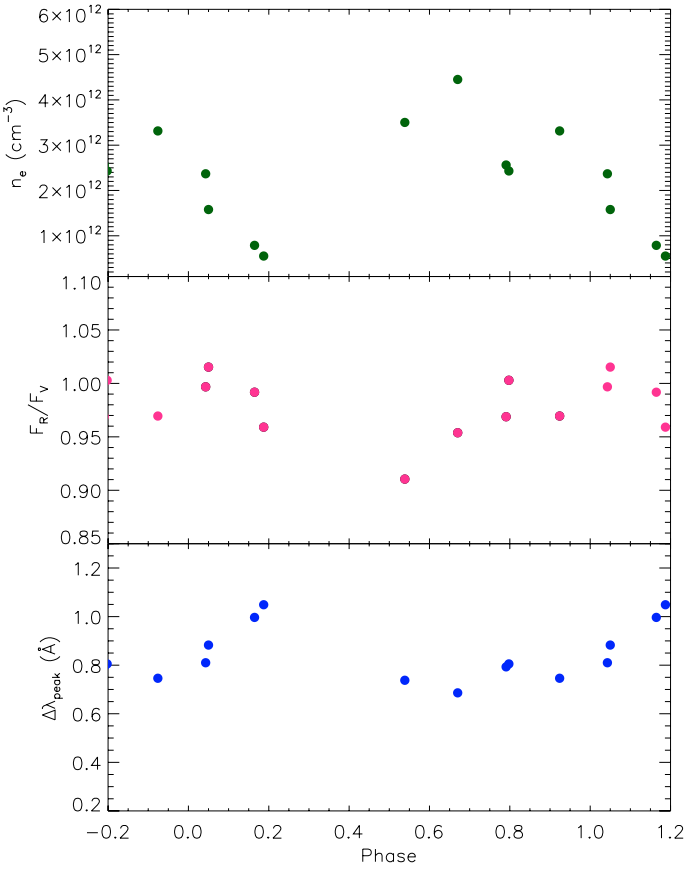

Fig. 2. *From top to bottom.* The computed electron density n_e (cm^{-3}), the flux ratio between the red and the blue peaks, and the peak separation in Å against the rotational phase.

The Hα equivalent width measured in the observed ($EW_{H\alpha}$) and in the residual spectra ($\Delta EW_{H\alpha}$), the radial velocity shifts of the Hα emission (ΔV_{em} and ΔV_{em}^{res}), and the contemporaneous light curve in the V band (from Paper I) are plotted in Fig. 3 as functions of the rotational phase. A remarkable anti-correlation of V brightness and Hα emission is apparent.

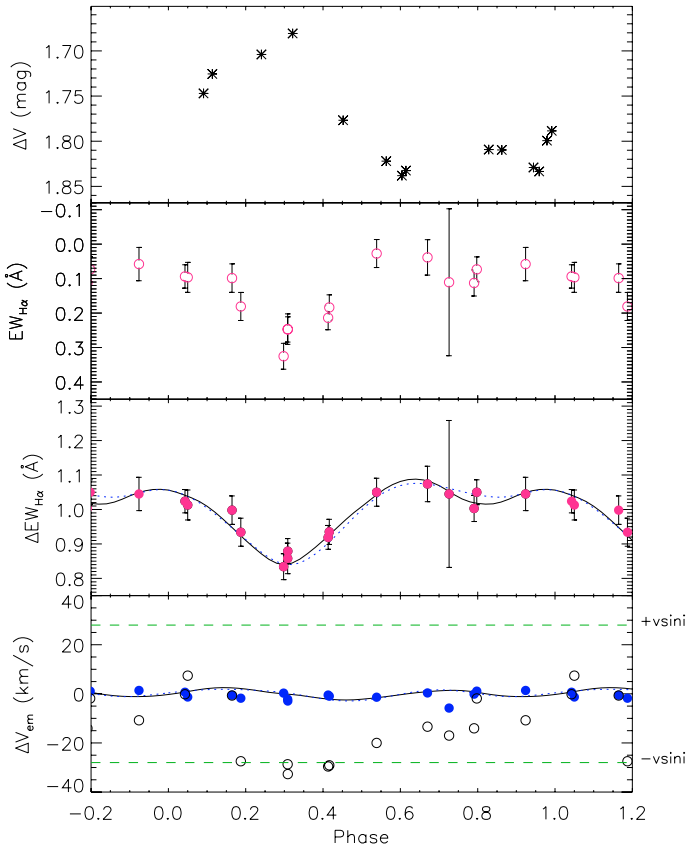

Fig. 3. *Top panel*: *V* light curve contemporaneous to the spectra. *Middle panels*: rotational modulation of the *raw* Hα equivalent width ($EW_{H\alpha}$, open circles) and of the *residual* Hα *EW* ($\Delta EW_{H\alpha}$, filled circles). *Bottom panel*: velocity shift between Hα emission and photospheric lines both for observed (open circles) and residual spectra (filled circles). The continuous lines in the *middle* and *bottom panels* represent the best fit of our 3-plage model (cf. Fig. 4), while the dotted lines represent the result of our 2-plage model.

The highest electron density is observed when the Hα line is strongest, indicating a denser chromosphere above more extended active regions, the opposite of what was observed in 1991 (Paper II). We also found an average value for the chromospheric electron density that was higher than the one reported in Paper II (2×10^{11} cm^{-3}). Moreover, the rotational modulation of all the quantities deduced by the Hα line analysis is much more evident in the present data. Presumably, in April–May 2000, LQ Hya was more active than in 1991, and it displayed more and larger active regions.

5. Discussion and conclusions

To obtain information about the surface location of the active regions in the chromosphere of LQ Hya, we applied a simple geometric *plage* model to the rotationally modulated chromospheric emission. This method had been described and successfully applied to the Hα modulation curves of several other active stars (e.g., Frasca et al. 2000; Biazzo et al. 2006; Frasca et al. 2008). On LQ Hya, two circular bright spots (plages) are normally sufficient for reproducing the observed variations within the data errors (cf. Frasca et al. 2000; Kővári & Bartus 2001). In our model the flux ratio between plages and the surrounding chromosphere ($F_{\rm plage}/F_{\rm chrom}$) is a free parameter. Solar values of $F_{\rm plage}/F_{\rm chrom} \approx 2$, as deduced from averaging many plages in Hα (e.g., Ellison 1952; LaBonte 1986; Ayres et al. 1986), are too low to model the high amplitudes of Hα ΔEW curves in very active stars (Biazzo et al. 2006; Frasca et al. 2008). In fact, extremely large plages, covering a significant fraction of the stellar surface, would be required with such a low flux ratio, and they could not reproduce the observed modulation. In order to achieve a good fit, a flux ratio of 5, which is also typical of the brightest parts of solar plages or of flare regions (e.g., Švestka 1976; Zirin 1988), was adopted.

The solutions essentially provide the longitude of the plages and give only rough estimates of their latitude and size. The information about the latitude of surface features can be recovered from the analysis of spectral-line profiles broadened by the stellar rotation, as we did for the spots of LQ Hya with Doppler imaging in Paper I. A similar technique cannot reach the same level of accuracy when applied to the Hα profile whose broadening is dominated by chromospheric heating effects, which are particularly efficient in the active regions (e.g., Lanzafame et al. 2000).

We searched for the best solution by varying the longitudes, latitudes, and radii of the active regions. The radii are strongly dependent on the assumed flux contrast $F_{\rm plage}/F_{\rm chrom}$. Thus, only the combined information between plage dimensions and flux contrast, i.e. some kind of plage "luminosity" in units of the quiet chromosphere ($L_{\rm plage}/L_{\rm quiet}$), can be deduced as a meaningful parameter. Note also that we cannot estimate the true quiet chromospheric contribution (network), since the Hα minimum value, $\Delta EW_{\rm quiet} = 0.84$ Å, could still be affected by a homogeneous distribution of smaller plages. However, such an approximation seems valid for LQ Hya because our aim was only to compare the spatial distribution of the main surface inhomogeneities at chromospheric and photospheric levels.

We also searched for solutions with three active regions, finding a small but possibly significant increase in the goodness of the fit, with the χ^2 passing from 5.77 to 4.45 (see Fig. 3). The model with only two plages requires features at rather high latitudes (Table 4) to explain the nearly flat and long-lasting maximum, while a 3-plage model allows placing plages at lower latitudes, in better agreement with the spot locations from Doppler imaging. However, the longitudes of the two largest plages do not change very much (less than 15 degrees).

The resulting plage longitudes are in good agreement with the Doppler results in Paper I; i.e., photospheric minima at 0.6 and 0.9 with the largest/coolest photospheric spots correspond to the most luminous chromospheric phases, and vice versa, the brightest photometric phase at 0.3 overlap with the lowest chromospheric Hα emission, again supporting the paradigm that photospheric spots are physically connected with chromospheric plages (Fig. 4).

The synthetic Hα *EW* curve for the model with three plages is plotted in the middle panel of Fig. 3 as a continuous line superimposed on the data (dots), while the 2-plage solution is displayed by a dotted line. Both of them reproduce the observed rotational modulation quite well. With the same models we were able to calculate the radial velocity shift between the Hα synthetic emission profile, resulting from the quiet chromosphere plus the visible plages, and the photosphere. It is clear in the bottom panel of Fig. 3 that the amplitude of the theoretical $\Delta V_{\rm em}$ curves, both for a 2-plage and a 3-plage model, is very low, consistent with the values derived from the residual profiles ($\Delta V_{\rm em}^{\rm res}$) and in total disagreement with the velocity shifts derived from the raw spectra. This strongly supports the spectral synthesis method we used to evaluate the chromospheric emission in the Hα line.

Table 4. Plage parameters for LQ Hya in April−May 2000.

Radius (°)	Lon. (°)	Lat. (°)	$\frac{F_{\rm plage}}{F_{\rm chrom}}$
2 Plages Solution			
15.5	215	35	5
20.0	353	66	5
3 Plages Solution			
13.0	210	20	5
13.0	8	15	5
9.5	280	15	5

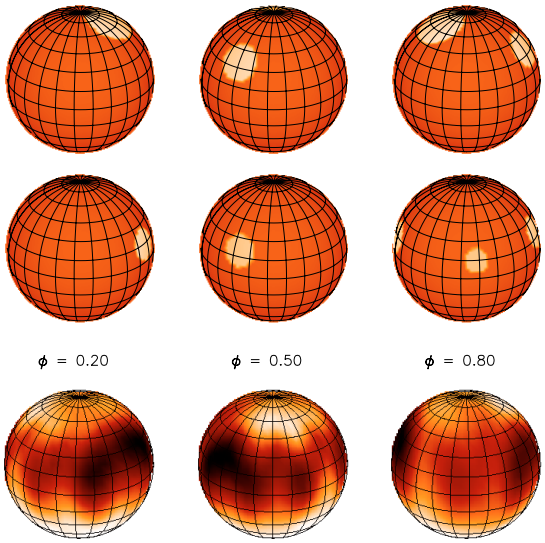

Fig. 4. Schematic representation of the surface features of LQ Hya in the chromosphere as reconstructed by the 2-plage (*top*) and by the 3-plage models (*middle*) and in the photosphere (*bottom*). In these maps, the star is rotating counterclockwise. Dominant features are found at similar longitudes at both chromospheric and photospheric levels.

We would like to outline the rotational modulation of other features observed in the Hα profile, such as the peak separation, which is related to the chromospheric electron density (Sect. 4) and the asymmetry of blue/red peak intensity (Fig. 2). The chromosphere of LQ Hya displays a higher electron density above active regions. The blue emission peak is stronger than the red one ($\frac{F_{\rm R}}{F_{\rm V}} < 1$) in the "quiet" chromosphere of LQ Hya, while nearly equal peaks ($\frac{F_{\rm R}}{F_{\rm V}} \simeq 1$) tend to be observed when the most active regions are in the visible hemisphere.

Asymmetry in the peaks of an emission line with a central reversal has been frequently observed for Ca II K line both in the Sun (e.g., Zirin 1988; Ding & Schleicher 1998, and reference therein) and in cool stars (e.g., Montes et al. 2000, and reference therein). The blue asymmetry is more frequently observed in the solar chromosphere and is commonly attributed to the propagation of acoustic waves (e.g., Cram 1976) with an upward velocity on the order of 10 km s^{-1} in the layer in which the K_2 emission peaks are formed or a downward motion in the layer producing the central reversal K_3 (e.g., Durrant et al. 1976).

Oranje (1983) has shown that the average Ca II K emission profile in solar plages has a completely different shape from the surrounding chromosphere, with the red peak slightly stronger than the blue one. This could reflect the different physical conditions and velocity fields in active regions compared to the quiet chromosphere. A similar analysis cannot be made for the Sun as a star in Hα, because this line is an absorption feature in the quiet chromosphere and only a filling in is observed in plages. However, similar changes of the Hα line profile can be expected in the plages of any stars that are more active than the Sun. Thus, the rotational modulation of $\frac{F_{\rm R}}{F_{\rm V}}$ is consistent with the presence of plages in the chromosphere of LQ Hya.

These results suggest scaled-up versions (regarding size and brightness) of solar-type plages for the Hα features observed in LQ Hya in 2000, without any clear evidence of strong mass motions in its chromosphere.

Acknowledgements. We are grateful to an anonymous referee for helpful comments and suggestions. This work has been partially supported by the Italian *Ministero dell'Università e Ricerca* (MUR), which is gratefully acknowledged. Zs.K. is a grantee of the Bolyai János Scholarship of the Hungarian Academy of Sciences and is also grateful to the Hungarian Science Research Program (OTKA) for support under grants T-048961 and K 68626. K.G.S. thanks the US Kitt Peak National Observatory for the possibility to record long time series of stellar data with the late Coudé-feed telescope, now retired.

References

Ayres, T. R., Testerman, L., & Brault, J. W. 1986, ApJ, 304, 542
Barden, S. C. 1985, ApJ, 295, 162
Biazzo, K., Frasca, A., Catalano, S., & Marilli, E. 2006, A&A, 446, 1129
Biazzo, K., Frasca, A., Henry, G. W., Catalano, S., & Marilli, E. 2007, ApJ, 656, 474
Bidelman, W. P. 1981, AJ, 86, 553
Catalano, S., Rodonò, M., Cutispoto, G., et al. 2000, in Kluwer Academic Publishers, Variable Stars as Essential Astrophysical Tools, ed. C. İbanoğlu, 687
Cram, L. E. 1976, A&A, 50, 263
Cram, L. E., & Mullan, D. J. 1979, ApJ, 234, 579
Ding, M. D., & Schleicher, H. 1998, A&A, 332, 767
Durrant, C. J., Grossmann-Doerth, U., &, Kneer, F. J. 1976, A&A, 51, 95
Ellison, M. A. 1952, MNRAS, 112, 679
Fekel, F. C., Moffett, T. J., & Henry, G. W. 1986, ApJS, 60, 551
Frasca, A., & Catalano, S. 1994, A&A, 284, 883
Frasca, A., Catalano, S., & Marilli, E. 1998, in The Tenth Cambridge Workshop on Cool Stars, Stellar Systems and the Sun, ed. J. A. Bookbinder, & R. A. Donahue (San Francisco: ASP), ASP Conf. Ser., 154, 1521
Frasca, A., Freire Ferrero, R., Marilli, E., & Catalano, S. 2000, A&A, 364, 179
Frasca, A., Biazzo, K., Taş, G., Evren, S., & Lanzafame, A. C. 2008, A&A, 479, 557
Heintz, W. D. 1981, ApJS, 46, 247
Herbig, G. H. 1985, ApJ, 289, 269
Kővári, Zs., & Bartus, J. 1997, A&A 323, 801
Kővári, Zs., Strassmeier, K. G., Granzer, T., et al. 2004, A&A, 417, 1047 (Paper I)
LaBonte, B. J. 1986, ApJS, 62, 241
Lanzafame, A. C., Busà, I., & Rodonò, M. 2000, A&A, 362, 683
Montes, D., Fernández-Figueroa, M. J., De Castro, E., & Cornide, M. 1995, A&AS, 109, 135
Montes, D., Fernández-Figueroa, M. J., De Castro, E., et al. 2000, A&AS, 146, 103
Oranje, B. J. 1983, A&A, 124, 43
Scarfe, C. D., Batten, A. H., & Fletcher, J. M. 1990, Publications of the Dominion Astrophysical Observatory Victoria, 18, 21
Strassmeier, K. G., Rice, J. B., Wehlau, W. H., Hill, G. M., & Matthews, J. M. 1993, A&A, 268, 671 (Paper II)
Strassmeier, K. G., Washuettl, A., Granzer, Th., Scheck, M., & Weber, M. 2000, A&AS, 142, 275
Švestka, Z. 1976, Solar Flares (Dordrecht: D. Reidel Publishing Company) , 7
Weis, E. W. 1996, AJ, 112, 2300
Zirin, H. 1988, Astrophysics of the Sun (Cambridge University Press), 214, 350